Application of Crop Model Data Assimilation With a Particle Filter for Estimating Regional Winter Wheat Yields

Zhiwei Jiang, Zhongxin Chen, Jin Chen, Jia Liu, Jianqiang Ren, Zongnan Li, Liang Sun, and He Li

***Abstract*—To improve the performance of crop models for regional crop yield estimates, a particle filter (PF) was introduced to develop a data assimilation strategy using the Crop Environment Resource Synthesis (CERES)—Wheat model. Two experiments involving winter wheat yield estimations were conducted at a field plot and on a regional scale to test the feasibility of the PF-based data assimilation strategy and to analyze the effects of the PF parameters and spatiotemporal scales of assimilating observations on the performance of the crop model data assimilation. The significant improvements in the yield estimation suggest that PF-based crop model data assimilation is feasible. Winter wheat yields from the field plots were forecasted with a determination coefficient (R^2) of 0.87, a root-mean-square error (RMSE) of 251 kg/ha, and a relative error (RE) of 2.95%. An acceptable yield at the county scale was estimated with a R^2 of 0.998, a RMSE of 9734 t, and a RE of 4.29%. The optimal yield estimates may be highly dependent on the reasonable spatiotemporal resolution of assimilating observations. A configuration using a particle size of 50, LAI maps with a moderate spatial resolution (e.g., 1 km), and an assimilation interval of 20 d results in a reasonable tradeoff between accuracy and effectiveness in regional applications.**

***Index Terms*—Crop model, data assimilation, leaf area index, particle filter (PF), remote sensing, yield estimation.**

I. Introduction

CROP YIELD information is required for sustainable agriculture management and national food security assessment, and it is critical that such data be determined on a regional scale in a timely and accurate manner [1]–[3]. However, traditional approaches to obtain regional crop yields typically suffer from the limitations of cost, timeliness, accuracy, and suitability on a regional scale. Recently, the rapid advancements of crop growth simulation [4] and observation technologies [5]–[7] have provided the ability to improve regional crop yield monitoring and forecasting. [8]. By making better use of crop growth models, crop growth processes can be effectively simulated under different environmental and management conditions while accounting for various limiting factors (e.g., soil, weather, water, and nitrogen) in a dynamic manner [9]. Nevertheless, improvements in simulation accuracy are often challenging when a crop model is used on a regional scale due to difficulties in obtaining regional model input and large uncertainties in regional parameters, including weather, soil, field management, crop cultivars, and other variables. The use of spatial observations from remotely sensed data is an ideal option for reducing regional simulation uncertainties [10]. Accordingly, data assimilation technologies with the advantage of integrating crop growth models with remote sensing information have been proposed and widely used in crop growth models such as World Food Studies (WOFOST) [11], Erosion Productivity Impact Calculator (EPIC) [12], and Decision Support System for Agro-technology Transfer (DSSAT) [13].

To date, several data assimilation strategies have been developed to reduce the discrepancy between observation and simulation by adjusting either the uncertain model parameters, initial conditions [14]–[18], or model state variables [19]–[21]. These strategies mainly include optimum estimation algorithms such as Shuffled Complex Evolution method developed at the University of Arizona (SCE-UA) [22], Simulated Annealing (SA) [23], POWELL [24], and sequential data assimilation algorithms, i.e., ensemble Kalman filter (EnKF) [25]. Early data assimilation strategies based on optimum estimation algorithms fail to consider errors in observations and the model itself. In addition, the iterative process of minimization between the modeled and observed values may require excessive computing time. Thus, the EnKF-based strategy that has a strong capacity for sequential data assimilation was introduced into crop growth simulations to alleviate the shortcomings of the optimum estimation algorithm. However, it should be noted that EnKF algorithm relies on the assumption that the posterior density at every time step is a Gaussian distribution parameterized by a mean and a covariance, resulting in an obvious deficiency when addressing complicated estimation issues in a realistic, nonlinear, and nonGausses dynamic system.

To address these problems associated with the EnKF algorithm, particle filters (PFs) have received increasing attention thanks to their improved performance in comparison to that of

Manuscript received November 05, 2013; revised January 08, 2014; accepted March 25, 2014. Date of publication April 23, 2014; date of current version January 06, 2015. This work was supported in part by the National Natural Science Foundation of China (Grant 41371396 and Grant 41301457); in part by the Agricultural Scientific Research Fund of Outstanding Talents and the Open Fund for the Key Laboratory of Agri-Informatics, Ministry of Agriculture, China (Grant 2013009); in part by Introduction of International Advanced Agricultural Science and Technology, Ministry of Agriculture, China (948 Program, 2011-G6); in part by National High Technology Research and Development Program of China (863 Program, Grant 2012AA12A307); and in part by the National Nonprofit Institute Research Grant of CAAS (IARRP-2014-14). (*Corresponding author: Z. Chen.*)

Z. Jiang is with the State Key Laboratory of Earth Surface Processes and Resource Ecology, Beijing Normal University, Beijing 100875, China, and also with the Key Laboratory of Agri-Informatics, Ministry of Agriculture, Institute of Agricultural Resources and Regional Planning, Chinese Academy of Agricultural Sciences, Beijing 100081, China (e-mail: zhiweijt@163.com).

Z. Chen, J. Liu, J. Ren, Z. Li, L. Sun, and H. Li are with the Key Laboratory of Agri-Informatics, Ministry of Agriculture, Institute of Agricultural Resources and Regional Planning, Chinese Academy of Agricultural Sciences, Beijing 100081, China (e-mail: chenzhongxin@caas.cn; liujia06@caas.cn; renjianqiang@caas.cn; lizongnan@aliyun.com; sunliang@caas.cn; lihe_caas@163.com).

J. Chen is with the State Key Laboratory of Earth Surface Processes and Resource Ecology, Beijing Normal University, Beijing 100875, China (e-mail: chenjin@bnu.edu.cn).

Color versions of one or more of the figures in this paper are available online at http://ieeexplore.ieee.org.

Digital Object Identifier 10.1109/JSTARS.2014.2316012

EnKF [26]. Similar to EnKF, PF is also a Monte Carlo technique that uses samples (i.e., particles) to estimate the underlying probability density function (PDF) of model states and parameters. However, in contrast with EnKF, PF can perfectly accommodate the propagation of nonGaussian distributions through nonlinear models. This approach has been successfully applied to studies on target tracking [27], hydrological parameter estimation and uncertainty analysis [28]–[32], and land surface processing simulations [33]–[36]. Accordingly, the PF-based strategy appears to be a better choice for complicated crop growth models, i.e., the Crop Environment Resource Synthesis (CERES)—Wheat model. Unfortunately, few studies on PF-based data assimilation for regional crop yield estimation have been published.

When PF-based crop model data assimilation is applied in an operational system for regional crop yield estimation, two problems must be addressed. First, the effect of PF parameters on the performance of crop model data assimilation should be determined. In theory, as the particle dimension increases or perturbation variance decrease, the probability distribution of the state particles may be much closer to the real state with a higher estimated accuracy [37]. However, the computing time will increase with increasing particle dimension. Hence, the reasonable parameters in a PF-based strategy must be provided as a tradeoff between accuracy and effectiveness in regional applications. Second, the effects of inadequate spatiotemporal resolution of remotely sensed productions (e.g., MODIS/LAI) [38], [39] on the performance of crop model data assimilation should be determined. Generally, a high frequency of observations is beneficial for reducing uncertainties in the simulation processes of crop models, although these satellite-based observations during the crop growing season are usually limited by frequent cloud coverage and long revisit periods. On the other hand, remotely sensed observations with a high-spatial resolution can provide more informative and higher quality observations [40], whereas this approach is problematic for large areas due to the high-computational effort required for data assimilation. Nevertheless, the effects of the spatio-temporal resolution of observations on the performance of data assimilation remain unclear, especially for PF-based crop model data assimilation.

The main objective of this study was to introduce the PF algorithm into crop model data assimilation and evaluate its performance. The CERES-Wheat model was employed to design a feasible data assimilation strategy with PF because the CERES-Wheat model is an outstanding agro-ecological dynamic model that considers the effects of weather, management, genetics, soil water, carbon, and nitrogen on crop yield simulations [41], [42]. Moreover, LAI observations were also used as an observational variable to couple observed LAI with simulated LAI. Two experiments for winter wheat yield estimations were performed in this study. One experiment was performed using the LAI measured on field plots; in this test, the feasibility of the data assimilation strategy was determined, and the effects of the PF parameters and the observation frequency on the data assimilation performance were evaluated. A second experiment was conducted that employed remotely sensed LAI with fine spatial resolutions on regional scale; in this case, regional winter wheat yields with different spatial resolutions were mapped, and the spatial scale effects of the LAI on the data assimilation performance were analyzed.

II. Methods

A. Particle Filter

The PF, which is a sequential Monte Carlo method, is a fully nonlinear filter with Bayesian conditional probability estimation [26]. The PF generates a probability-weighted posterior sample set (also called particles) through the direct evaluation of the Bayesian formula at each prior sample point to approximate the posterior PDF. In comparison with the well-known EnKF, this evaluation does not restrict the probability distribution of the prior sample and the observation as Gaussian [43]. In principle, PF can be used for any recursive estimation or probability reasoning of nonlinear, nonGaussian dynamic systems [44].

Schematically, the PF may be viewed as a combination of two main elements, namely, sequential importance sampling (SIS) and resampling [45]. SIS is used to select the particle weights based on the fact that direct sampling from the target density (posterior), which is often nonGaussian, is generally difficult (if not impossible). To avoid this difficulty, importance sampling generates particles from a known function called a proposal distribution (or importance density) and assigns the weights (importance weights). A sequential update to the important weights for each iteration is then achieved by factorizing the proposal distribution [32]. A resampling algorithm is mainly used to avoid the degeneracy of the SIS method, eliminate samples with low weights, and multiply samples with high importance weights while keeping the total number of particles unchanged [46]. Resampling involves selecting new particle positions and weights such that the discrepancy between the resampled weights is minimized [45]. Several resampling algorithms have been proposed, such as importance sampling resampling [47], residual resampling (RR) [48], stratified resampling [49], multinomial resampling [45], and systematic resampling [26]. In this present study, the RR algorithm was employed because of its lower computational cost and smaller variance in comparison to the other resampling schemes.

B. Crop Growth Model

The CERES-Wheat model was developed and integrated into DSSAT software in an International Benchmark Sites for Agrotechnology Transfer project sponsored by the United States Department of Agriculture [13]. Driven by input data on weather, soil, field management, and genetic information, the CERES-Wheat model can simulate daily phenological development, vegetative and reproductive plant development stages as well as assimilate partitioning, the growth of leaves and stems, senescence, biomass accumulation, and root system dynamics under stressful environments, i.e., those involving light, temperature, water, nitrogen, carbon, and field management interventions [15]. The water and nitrogen sub-models cause feedback effects on plant growth and development. This model has been widely applied to field sites to assess crop potential productivity [50], [51], and the influence of climate change on grain yields [41], [42], farmland water, and fertilizer management [52], as well as for other purposes.

To obtain accurate predictions, a model calibration is first performed, i.e., an estimation of the cultivar characteristics using field winter wheat experimental data. In this study, *in situ* data for the study area were employed to estimate the genetic coefficients in the CERES-Wheat model such that differences between the

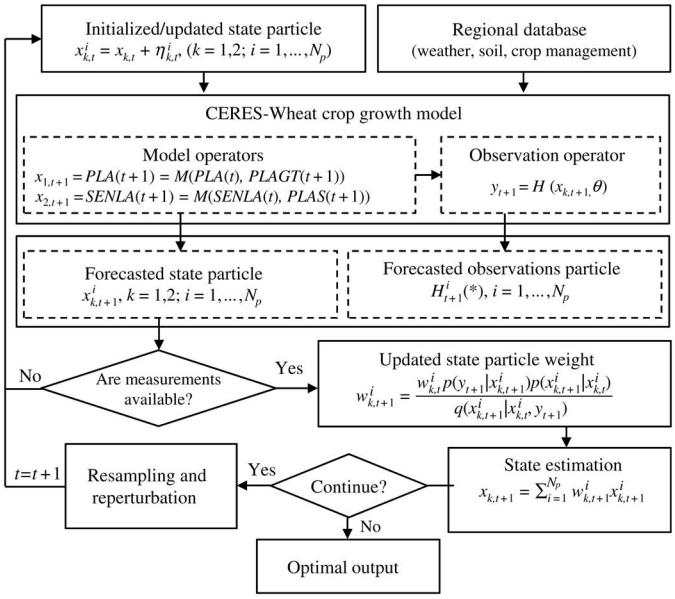

Fig. 1. Flowchart for the PF-based CERES-Wheat model data assimilation.

simulated and measured values were minimized to within acceptable error limits.

C. Crop Model Data Assimilation Strategy

A sequential data assimilation strategy based on the residual resampling particle filter (RRPF) was designed to sequentially correct the simulation process of the CERES-Wheat model using the observed data to achieve the optimal estimation of crop yield. A full description of the assimilation process is given below and illustrated in Fig. 1.

1) Model operator and observation operator. For a discrete-time dynamic state-space model, the current state of the dynamic system is only associated with the state at the previous time, and its evolution can be formulated as follows [46]:

$$x_{k,t+1} = M\left(x_{k,t}, \theta, u_{k,t}\right) + \eta_{k,t+1} \quad (1)$$

$$y_{t+1} = H\left(x_{k,t+1}, \theta\right) + \varepsilon_{t+1} \quad (2)$$

where $x_t \in \Re^{k \times N_x}$ denotes the $k \times N_x$ dimensional state vector of the system at time t with the initial PDF, which evolves over time as a first-order Markov process according to the conditional PDF $p(x_{k,t+1}|x_{k,t})$. The $\mathrm{N_y}$ dimensional observation vector $y_{t+1} \in \Re^{N_y}$ is conditionally independent given $x_{k,t+1}$, and the observation in (2) is represented by the PDF $p(y_{t+1}|x_{k,t+1})$. Nonlinear operators $M(\cdot)$ and $H(\cdot)$ express the system transition in response to forcing data $\mathrm{u_t}$, time invariant model parameters θ, and the forecasted state variables. Independent random vectors $\eta_{k,t+1}$ and ε_{t+1} represent the model and the measurement error and consist of a white noise sequence with a mean of zero and a variance of $Q_{k,t+1}$ and R_{t+1}, respectively.

In the CERES-Wheat model, the LAI at time t is described as a function expressing the plant leaf area (*PLA*) and senesced leaf area (*SENLA*) (3). PLA is a cumulative time function related to the plant area growth (*PLAGT*) (4), and *SENLA* is a cumulative time function of plant area senescence caused by metabolism, cold, tillers, and stress. Hence, *PLA* and *SENLA* are regarded as state variables whose integrating functions forward with time are considered to be model operators. The LAI function was used as an observational operator in the data assimilation process

$$y_{t+1} = LAI(t+1) = H(x_{k,t+1}, \theta), \quad k = 1, 2 \quad (3)$$

$$\begin{aligned} x_{1,t+1} &= PLA(t+1) \\ &= M(PLA(t), PLAGT(t+1)) \end{aligned} \quad (4)$$

$$\begin{aligned} x_{2,t+1} &= SENLA(t+1) \\ &= M(SENLA(t), PLAS(t+1)) \end{aligned} \quad (5)$$

where LAI is the winter wheat leaf area index, PLA is the plant leaf area, SENLA is the senesced leaf area, PLAGT is the growth plant area, and PLAS is the reduced leaf area because of various stress factors.

2) Initialization of model state variables and forecast. The model state variables $PLA(t)$ $(= x_{1,t})$ and $SENLA(t)$ $(= x_{2,t})$ were perturbed by using the Monte Carlo method to sample the white noise $\eta^i_{k,t}$ from a uniform distribution for Np particles, where $k = 1, 2$, $i = 1, \ldots, Np$; then, the particles at time t can be resampled as $x^i_{k,t} = x_{k,t} + \eta^i_{k,t}$, where $k = 1, 2$, $i = 1, \ldots, Np$. Each particle was uniformly assigned the weight as $w^i_k = 1/Np$.

With initial particles of model state variables at time t, the CERES-Wheat model propagates Np model states $x^i_{k,t}$ forward in time to obtain the model predicted state $x^i_{k,t+1}$. Correspondingly, the forecasted observation particles $H^i_{t+1}(\cdot)$ were obtained using the observation operator $H(\cdot)$.

3) Update model states weights. Particle weights $w^i_{k,t+1}$ were updated using forecasted observations $H^i_{t+1}(\cdot)$ and measured observations y_{k+1} at time $t+1$ according to (6) [32], [37], [46]:

$$w^i_{k,t+1} = \frac{w^i_{k,t} p(y_{t+1}|x^i_{k,t+1}) p(x^i_{k,t+1}|x^i_{k,t})}{q(x^i_{k,t+1}|x^i_{k,t}, y_{t+1})} \quad (6)$$

where $q(x^i_{k,t+1}|x^i_{k,t}, y_{t+1})$ denotes the posterior PDF, which is an important term because it significantly influences the filter performance [46]. Generally, the prior transition is used as the proposal distribution, where

$$q\left(x^i_{k,t+1}|x^i_{k,t}, y_{t+1}\right) = p(x^i_{k,t+1}|x^i_{k,t}). \quad (7)$$

The weight updating then simplifies to

$$w^i_{k,t+1} = w^i_{k,t} p(y_{t+1}|x^i_{k,t+1}). \quad (8)$$

In this study, we elected to use Gaussian error distributions for all observation perturbations, partly for simplicity, partly because we have no knowledge of the appropriate distribution to use, and partly because a random

perturbation with Gaussian distributions does not yield unrealistic results. A Gaussian observation noise with variance R_k was assumed [26], [32], [53]–[55]. Thus, the likelihood estimation can be expressed as

$$L(y_{t+1}|x^i_{t+1}) = \frac{1}{(2\pi)^{\frac{1}{2}}|R_{t+1}|^{\frac{1}{2}}} \times exp\left[-\frac{1}{2R_{t+1}}\left(y_{t+1} - H^i_{t+1}(\cdot)\right)^2\right]. \quad (9)$$

Finally, the updated particle weights were obtained according to

$$w^i_{k,t+1} = \frac{exp\left[-\frac{1}{2R_{t+1}}\left(y_{t+1} - H^i_{t+1}(\cdot)\right)^2\right]}{\sum_{i=1}^{N_p} exp\left[-\frac{1}{2R_{t+1}}\left(y_{t+1} - H^i_{t+1}(\cdot)\right)^2\right]}. \quad (10)$$

Consequently, the model state at time $\mathrm{t}+1$ can be approximated by

$$x_{k,t+1} = \sum_{i=1}^{N_p} w^i_{k,t+1} x^i_{k,t+1}. \quad (11)$$

4) Residual resampling. In this algorithm, for $i = 1, \ldots, Np$, we set $K_{k,i} = \lfloor N_p w^i_{k,t+1} \rfloor$, where the operator $\lfloor \cdot \rfloor$ takes the integer part of its argument. The normalized residual weights $w^i_{k,t+1,res}$ were then calculated according to

$$w^i_{k,t+1,res} = \frac{N_p w^i_{k,t+1} - K_{k,i}}{N_p - \sum_{i=1}^{N_p} K_{k,i}}. \quad (12)$$

Normalized residual weights $\mathrm{w^i_{k,t+1,res}}$ were subsequently used to construct an empirical cumulative distribution function and sample $\mathrm{N_p} - \sum_{\mathrm{i=1}}^{\mathrm{N_p}} \mathrm{K_{k,i}}$ times to obtain the remaining particles. The resampling process was performed according to [26] and [32].

5) Perturbation of resampled particles. With all PFs, resampling may be used to avoid the problem of degeneracy. However, resampling can lead to sample impoverishment, or lack of particle diversity, especially if the process noise is low under strong constraints in a dynamic system [29], [31]. Hence, a reperturbation of the resampled particle was conducted with parameterizing error η' as a function of the resampled state $\mathrm{x_{k,t+1,res}}$ as follows, similar to [56].

$$x^i_{k,t+1,rep} = x_{k,t+1,res} + \eta'_{k,t+1}$$
$$\eta'_{k,t+1} \sim N(0, (\varepsilon_{rep} x_{k,t+1,res})^2) \quad (13)$$
$$x_{k,t+1,res} = \sum_{i=1}^{N'_p} w^i_{k,t+1,res} x^i_{k,t+1,res} \quad (14)$$

where $x^i_{k,t+1,rep}$ is the ith reperturbed state particle at time $k+1$, η' is the random noise with a mean of zero and a variance of $(\varepsilon_{rep} x_{k,t+1,res})^2$, ε_{rep} is a parameter that must be specified, $x_{k,t+1,res}$ is a weighted approximation to the resampled particle, and N'_p is the truncated number of resampled particles, $N'_p \leq N_p$.

6) Assimilating process control. The updated state particle is input as the initial state particle during the next evolutionary cycle until all available observations are assimilated into the CERES-Wheat model. The process of data assimilation then stops and outputs the optimal estimated yield.

D. Assimilation Experiments for Winter Wheat Yield Estimation

To introduce the PF algorithm into the crop model data assimilation and evaluate its performance, two experiments for winter wheat yield estimation were performed in this study. One experiment at the field scale was carried out to illustrate the feasibility of a data assimilation strategy and to evaluate the effects of PF parameters and the observation frequency on data assimilation performance. Another experiment conducted on a regional scale was used to map regional winter wheat yields and analyze the spatial scale effects of remotely sensed LAI maps on data assimilation performance.

For the experiments at the field scale, the *in situ* data for the field plots were first employed to test the feasibility of the data assimilation strategy. Subsequently, crop model data assimilation experiments with the state particle size set to 10, 50, 90, 130, and 170 and the parameter of state particle variance ε_{rep} set to 1/2, 1/3, 1/4, 1/5, and 1/6 were performed to evaluate the effects of both the state particle size and the perturbed variance on yield estimations. In addition, experiments that assimilated measured LAI with equal time intervals of 8, 14, 20, 26, and 32 d were also performed to determine the uncertainties in the yield estimations for a different combination of the LAI values measured during the winter wheat growing season.

For the regional-scale experiments, regional winter wheat yields were mapped using remotely sensed LAI maps with pixel sizes of 30, 300, 600, 900, 1200, 1500, 1800, and 2100 m. The spatial scale effects of the LAI maps on performance of data assimilation were then analyzed. In these experiments, the time interval of the assimilated observation was 11 d, the dimension of the state particle was 50, the parameter ε_{rep} for reperturbed state particle was 1/6, and other settings were identical to field-scale experiments.

In the data assimilation experiments described above, the crop management parameters in the CERES-Wheat model were set using the regional mean value. The planting date was October 10, 2008, the sowing population was 450 plants per square meter, and the row spacing was 15 cm. Irrigation at a volume of 65 mm was conducted three times on March 10, April 1, and May 10 of the following year. The nitrogen fertilizer volume was 120 kg/ha. The soil and weather parameters were derived from field observations.

III. Study Area and Data

A. Study Area

Hengshui (37°03′–38°23′N; 115°10′–116°34′E), the primary planting area for winter wheat, is located in the Huang-Huai-Hai

Plain of China. This area has a temperate sub-humid continental monsoon climate. The annual average temperature is between 12 °C and 13 °C, the annual cumulative temperature above 0 °C is between 4 200 °C and 5 500 °C, the annual average precipitation is between 500 and 900 mm, the annual cumulative radiation is between 5.0×10^3 and 5.2×10^3 $\mathrm{MJ/m^{-2}}$, and the frost-free season lasts between 170 and 220 d. There are abundant water resources, with nine tributaries belonging to four rivers of the Haihe River system. In this region, the anthropogenic soil types were generally categorized as fluvo-aquic soil, sandy fluvo-aquic soil, wet fluvo-aquic soil, salinized fluvo-aquic soil, and meadow saline soil. The main vegetation includes crops such as winter wheat, maize, and cotton. For winter wheat, the developmental period occurs from early October to early June of the next year. The re-greening period begins in early March, the heading stage lasts from the end of April until early May, and the harvest usually occurs in mid-June.

B. Regional Soil, Weather, and Crop Information

The soil map for the study area was derived from the Soil and Terrain database for primary Chinese data at a scale of 1:1 million; this map was compiled using enhanced soil information within the framework of the FAO's Land Degradation Assessment in Drylands (LADA) program (http://www.isric.org/data/soil-and-terrain-database-china). Data on the physical and chemical properties of the soil profiles were collected from the Soil Species of Hebei Province [57].

Meteorological data were derived from the National Meteorological Information Center, China Meteorological Administration (http://cdc.cma.gov.cn/), and included a daily estimation of maximum and minimum temperatures, precipitation, sunshine hours, wind speed, and relative humidity. In addition, radiation was estimated at the station level based on sunshine duration [58]. In this study, daily meteorological parameter data for the study area were interpolated as a raster map with grid cells using ANUSPLIN software [59].

Detailed crop management information was also surveyed, including the dates of planting and harvest, planting depth and spacing, planting density, irrigation dates and volumes, fertilization date and volume, phenological calendar, and other data. Winter wheat yield data were measured at 53 field plots, and the regional statistical yields for 11 counties were obtained from the Hebei Rural Statistic Yearbook (2010) [60].

C. Remotely Sensed LAI Maps

Remotely sensed images with four bands (blue, green, red, and near-infrared) at a 30-m spatial resolution were acquired from the Environment and Disaster Monitoring and Forecasting based on the Small Satellite Constellation A and B satellites (HJ-1A/B satellites) (http://www.cresda.com/n16/index.html) from March to June of 2009. A series of pre-processing step was performed using ENVI software [61] and included radiometric calibration, atmospheric correction, and geometric correction to convert HJ CCD radiance to reflectance with the correct geographic information.

To extract regional winter wheat LAI maps, A Two-Layer Canopy Reflectance Model (ACRM) [62] was employed to establish the Lookup Table (LUT) [63]. To avoid an ill-posed inversion, the estimated LUT was regularized according to the image statistical information and a priori knowledge from winter wheat observations. To eliminate inversion distortion from clouds, moisture, aerosols, and mixed pixels, a Savitzky-Golay filter [64], [65] was used to smooth the time series of the LAI maps. Finally, acceptable LAI maps of winter wheat were extracted with a R^2 of 0.82, a RE of 10.75%, and a root-mean-square error (RMSE) of 0.46.

IV. Results

A. Experiments for Winter Wheat Yield Estimations at the Field Scale

1) Winter Wheat Yield Estimation at the Field Scale: Initial parameters and conditions concerning soil, weather, and crop management were significantly different and were difficult to collect on a regional scale. There were often many uncertainties regarding the simulation in CERES-Wheat if a general model was configured for the study area, especially for aspects of crop management such as planting, irrigation, and fertilization. These factors led to lower accuracy in regional crop growth simulation and yield estimations [Fig. 2(a) and (b)], which limited the potential application of the crop model. To improve the accuracy of the yield estimation, the PF-based data assimilation strategy was first introduced to improve the CERES-Wheat simulation process. The incorporation between the observed and modeled LAIs was performed under the dynamic framework of the winter wheat growth process such that the LAI simulation was sequentially optimized, which led to an optimal yield estimation. A series of LAIs measured at 53 field plots were assimilated into CERES-Wheat. Consequently, the yield estimations were dramatically improved, with a R^2 of 0.87, a RMSE of 251 kg/ha, and a RE of 2.95% [Fig. 2(c)]. The LAI simulated more closely agreed with the actual LAI, with a R^2 of 0.95, a RMSE of 0.39, and a RE of 8.56% [Fig. 2(d)]. The experimental results support the technical and practical feasibility of a PF-based crop model data assimilation.

2) Effects of PF Parameters on the Yield Estimation: In the PF data assimilation, the residual resampling and reperturbation were performed to improve the selection of the model state samples in an appropriately representative and diverse manner. The optimal yield estimates also support the improvements on impoverishment and diversity of resampled particles by employing a lower dimension of state particles and consuming less computing time. As shown in Fig. 3(a), there was not a substantial improvement in the yield estimation as the model state particle increased, although the computing cost increased several-fold. The accuracy of winter wheat yield estimations tended to slightly improve as the particle dimension increased: the normalized RMSE (NRMSE) decreased from 3.54% (for a particle dimension of 10) to 3.43% (for a particle dimension of 170), the RE correspondingly decreased from 3.02% to 2.95%, and the computing time needed to complete a yield estimation increased from 8.20 to 134.77 s.

With increasing perturbing variance, the local diversity of the state particle was somewhat reduced, which resulted in the increasing error of the analysis state and, consequently, a loss of accuracy in the data assimilation of yield estimation. Nearly, identical yield estimation accuracies (RE 2.92%–2.98%, NRMSE 3.39%–3.49%) were obtained when the parameter ε_{rep} of perturbing variance increased from 1/6 to 1/3

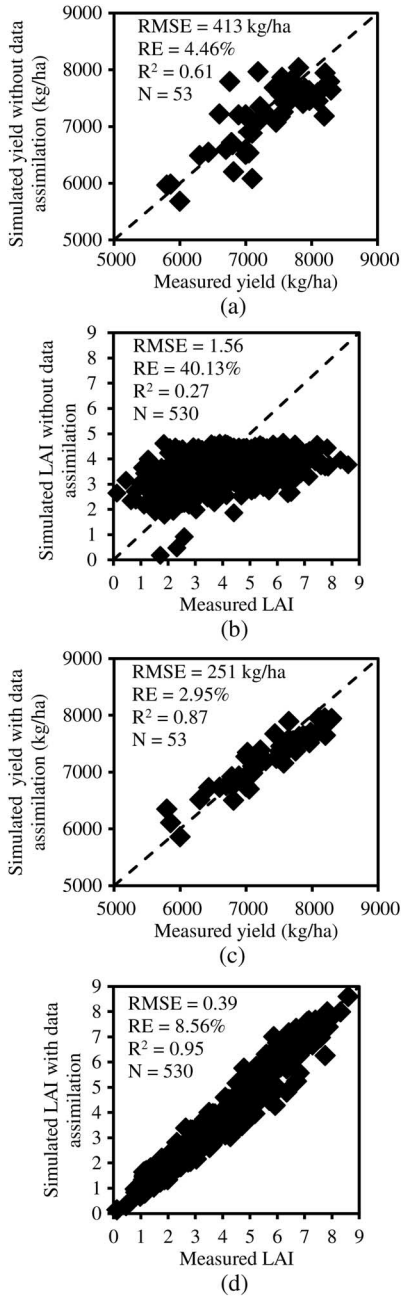

Fig. 2. Estimated yield and LAI of winter wheat with no data assimilation (a, b) and with the PF-based data assimilation (c, d).

[Fig. 3(b)]. However, there appeared to be a clear decreasing trend when the parameter ε_{rep} of perturbing variance increased to half the state value ($\mathrm{RE} = 4.59\%$, $\mathrm{NRMSE} = 6.92\%$).

3) Effects of the Assimilated Observation Frequency on the Yield Estimation: The assimilation of the LAI observed during the growing season could effectively correct the simulated trajectory of LAI in CERES-Wheat, especially with respect to shifts and underestimates of the LAI top value during the booting and flowering stages. Hence, modest increases in the frequency of assimilating observations may improve yield estimations. The experimental results showed that the accuracy of the yield estimation tended to significantly improve as the frequency of assimilating LAI increased from 26 to 8 d, the NRMSE dropped from 5.63% to 3.43%, and the RE decreased from 3.78% to

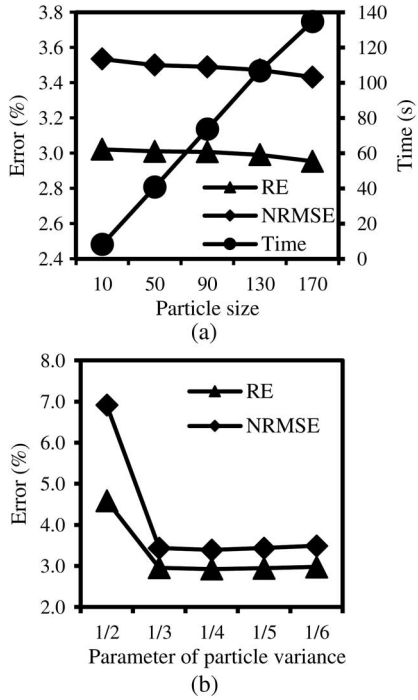

Fig. 3. Performance of data assimilation for different PF parameters.

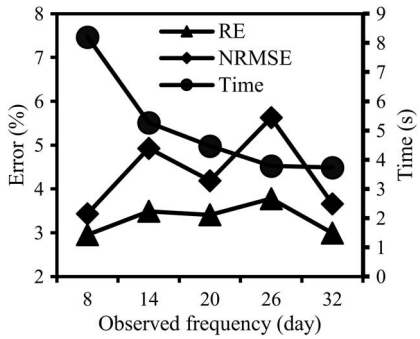

Fig. 4. Performance of data assimilation for different frequencies of assimilating observations.

2.95% (Fig. 4). A comparison of the accuracy of yield estimations with the assimilating observation interval of 26 d (Julian days 76, 102, and 128) showed that a more effective adjustment of the simulating process was achieved using the observed LAI with a frequency of 32 d (Julian days 76, 108, and 140), which more accurately described the typical state change during winter wheat growing season over field plots, leading to the better yield estimation despite a lower frequency of assimilating observations.

In addition, as the assimilating observation frequency decreased, the computing time clearly decreased from 8.20 s (for an assimilating observation frequency of 8 d) to 3.73 s (for an assimilating observation frequency of 32 d) for the data assimilation process of the yield estimation for a field plot (Fig. 4).

B. Experiments for Winter Wheat Yield Estimations on a Regional Scale

Remotely sensed LAI maps with a spatial resolution of 30 m were used to map regional winter wheat yields. The yield map

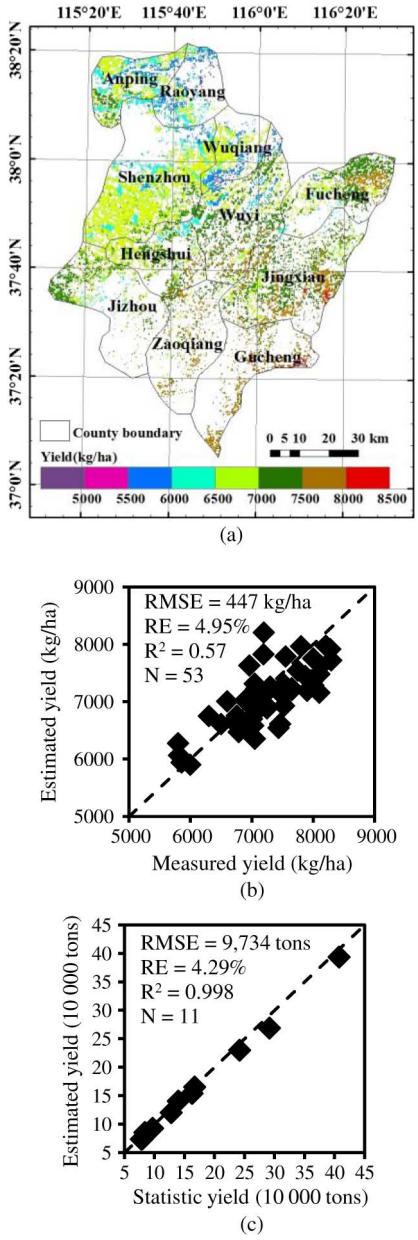

Fig. 5. Winter wheat yield map with a resolution of 30 m × 30 m and an accuracy evaluation. (a) Yield map with spatial resolution of 30 m. (b) Yield estimation in pixel. (c) Global yield estimation in county.

shows that the yield per unit area tended to decrease from the northwest to the southeast of Hengshui [Fig. 5(a)]. The average yield over the study region was 6716 kg/ha, the yield range was 5039 to 8324 kg/ha, and the coefficient of variation was 0.14. The winter wheat yield of 94.82% was between 5759 and 7813 kg/ha. The maximum productive capacity was observed in Gucheng county (7723 kg/ha) followed by Wuqiang (7481 kg/ha) and Jingxian (7335 kg/ha). The minimum yield was 6112 kg/ha in Raoyang.

An accuracy verification was performed on a pixel scale and on a county scale. The estimated yields of 53 pixels better corresponded to the actual yields of field plots, with a R^2 of 0.57, a RMSE of 447 kg/ha, and a RE of 4.95% [Fig. 5(b)]. The statistic results of yields for 11 counties showed that the R^2 was 0.998, the RMSE was 9734 t, and the RE was 4.29% [Fig. 5(c)].

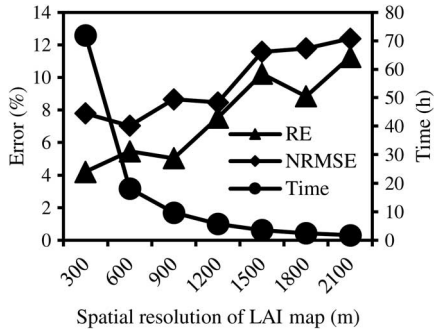

Fig. 6. Performance of data assimilation for different spatial resolutions for assimilating LAI maps.

In general, as the spatial resolution of the assimilated LAI maps decreased from 300 to 2100 m, the spatial distribution detail of the yields showed a remarkable roughness; in addition, the accuracies tended to decrease, and the RE and NRMSE decreased from 4.19% and 7.78% to 11.26% and 12.38%, respectively (Fig. 6). Specifically, when the spatial resolution of the LAI maps decreased from 300 to 1200 m, equivalent yield accuracies were obtained for the average changing rates with a RE and NRMSE of 0.59% and 1.49%, respectively. As the spatial resolutions of the LAI maps decreased from 1500 to 2100 m, the yield estimation accuracies dropped sharply in concert with a fluctuation in the uncertainty. In these scenarios, the average decreases in the RE and NRMSE were 2.19% and 1.17%, respectively. The decreasing trend in the computing time was fitted by a power-exponent model, and the time was reduced from 71.89 to 1.79 h.

V. Discussion and Conclusion

Crop model data assimilation is a promising approach for monitoring crop growth and predicting crop yield on a regional scale [19]. Alternatively, dynamic agroecosystem models can be used to simulate temporal changes according to the climate-soil-crop-management system of diagnosing and forecasting crop growth status during different developmental stages. On the other hand, remote sensing can provide actual information on regional crop growing states in real time. Each of these technologies addresses the shortcomings of the other to accurately and efficiently estimate crop yields on a regional scale. The experimental results in this work showed that significant improvements in yield estimation were observed on a field plot and on a regional scale when the measured LAIs as well as remotely sensed LAI maps were assimilated. In addition to the yield, other critical information on regional crop growth may also be estimated, including the biomass, harvest index, soil organic nitrogen, organic carbon, and evapotranspiration. These results suggest that crop model data assimilation is feasible and has a potential application in operational systems for monitoring regional crops in the near future.

In this study, PF was first introduced to design the data assimilation strategy within the CERES-Wheat model. The PF has been successfully applied in data assimilation with a process-based agroecological model due to its strong ability to address nonlinearity and nonGaussian issues [66]. PF can sample particles and update particle weights according to any distribution function. The use of a resampling and reperturbation of resampled particles in our strategy can effectively multiply

particles with high-importance weights and avoid a lack of particle diversity under the constraints of a dynamic system by using fewer particles. In addition, compared to a traditional four-dimensional variation strategy [67], the PF-based data assimilation strategy is able to express the model estimation as a recursive process that avoids the higher dimensions of control variables and a high-computational burden. The experimental results presented here also support the strong performance of the PF in the case of nonlinear agroecosystems. When the measured LAIs were assimilated at a field plot, the R^2 of the forecasted yields was 0.87, the RMSE was 251 kg/ha, and the RE was 2.95%. When remotely sensed LAI maps were assimilated on a county scale, the R^2, RMSE, and RE of the forecasted yields were 0.998, 9734 t, and 4.29%, respectively.

Unfortunately, few studies have focused on the application of PF-based crop model data assimilation to yield estimations. In this work, the uncertain effects of the PF parameters and spatio-temporal scales of assimilating observation were given greater emphasis. The experimental results showed that the particle dimension and perturbing variance in PF appear to be not significantly sensitive to the accuracy of yield estimation because of a reperturbation of resampled particles, especially when the particle dimension increased above a certain threshold value, which is of great significant for regional applications. The optimal yield estimates may be highly dependent on the reasonable spatiotemporal resolution of assimilating observations, which implies an uncertainty of remotely sensed data in a grid. Observations with a high temporal and spatial resolution may significantly improve the accuracy of crop yield estimations, although the increased computing time may be problematic for regional applications. In our study, the use of PF-based CERES-Wheat model data assimilations with an ensemble size of 50, LAI maps with moderate spatial resolution (e.g., 1 km), and assimilation interval of 20 d appears to be a reasonable tradeoff between accuracy and effectiveness in regional applications.

In addition to the factors assessed in our study, other uncertain elements, e.g., the soil, weather, regional field management information, multi-source remotely sensed observations, and perturbations of observational errors with possibly unknown distributions, may also lead to a poor performance of crop model data assimilation. Unfortunately, the analysis of these problems has received little attention in previous studies. These uncertainties will be analyzed in our further research. To achieve this goal, the methods of improving the observational perturbation and resampling state particle [28], [29], the strategies of simultaneous state-parameter estimation [21], [32], [68], multi-source data assimilation [69], and ensemble-based four-dimensional variational algorithms [70]–[72], will be introduced to improve the performance of crop model data assimilation. In the coming years, significant advances in remote sensing technologies may improve upon vegetation products (e.g., LAI) [73]–[75], especially addressing limitations in temporal and spatial resolutions due to the limits of the revisit circle, cloud coverage and/or mixed-pixel errors [76]. All of these factors will lead to new advances and challenges in our future work.

References

[1] J. M. Slingo, A. J. Challinor, B. J. Hoskins, and T. R. Wheeler, "Introduction: Food crops in a changing climate," *Philos. Trans. Roy. Soc. Lond. B Biol. Sci.*, vol. 360, no. 1463, pp. 1983–1989, Nov. 2005.

[2] M. W. Rosegrant and S. A. Cline, "Global food security: Challenges and policies," *Science*, vol. 302, pp. 1917–1919, 2003.

[3] D. S. Battisti and R. L. Naylor, "Historical warnings of future food insecurity with unprecedented seasonal heat," *Science*, vol. 323, no. 5911, pp. 240–244, Jan. 2009.

[4] P. B. Alton, "From site-level to global simulation: Reconciling carbon, water and energy fluxes over different spatial scales using a process-based ecophysiological land-surface model," *Agric. Forest Meteorol.*, vol. 176, pp. 111–124, Jul. 2013.

[5] C. Yang, J. H. Everitt, Q. Du, B. Luo, and J. Chanussot, "Using high-resolution airborne and satellite imagery to assess crop growth and yield variability for precision agriculture," *Proc. IEEE*, Mar. 2013, vol. 101, no. 3, pp. 582–592.

[6] W. G. M. Bastiaanssen, D. J. Molden, and I. W. Makin, "Remote sensing for irrigated agriculture: Examples from research and possible applications," *Agric. Water Manage.*, vol. 46, no. 2, pp. 137–155, Dec. 2000.

[7] A. F. H. Goetz, "Three decades of hyperspectral remote sensing of the Earth: A personal view," *Remote Sens. Environ.*, vol. 113, no. 1, pp. S5–S16, Sep. 2009.

[8] B. Luo, C. Yang, J. Chanussot, and L. Zhang, "Crop yield estimation based on unsupervised linear unmixing of multidate hyperspectral imagery," *IEEE Trans. Geosci. Remote Sens.*, vol. 51, no. 1, pp. 162–173, Jan. 2013.

[9] M. Launay and M. Guerif, "Assimilating remote sensing data into a crop model to improve predictive performance for spatial applications," *Agric. Ecosyst. Environ.*, vol. 111, no. 1–4, pp. 321–339, Dec. 2005.

[10] W. D. Batchelor, B. Basso, and J. O. Paz, "Examples of strategies to analyze spatial and temporal yield variability using crop models," *Eur. J. Agron.*, vol. 18, no. 1–2, pp. 141–158, Dec. 2002.

[11] R. J. Hijmans, I. M. Guiking-Lens, and C. A. van Diepen, "System description of the WOFOST 6.0 crop simulation model implemented in CGMS. Volume 1: Theory and algorithms," EUR 15956. Luxembourg: Office for Official Publications of the European Communities, p. 146, 1994.

[12] J. R. Williams, C. A. Jones, J. R. Kiniry, and D. A. Spanel, "The EPIC crop growth model," *Trans. ASABE*, vol. 32, no. 2, pp. 497–511, 1989.

[13] J. W. Jones, G. Hoogenboom, C. H. Porter, K. J. Boote, W. D. Batchelor, L. A. Hunt, P. W. Wilkens, U. Singh, A. J. Gijsman, and J. T. Ritchie, "The DSSAT cropping system model," *Eur. J. Agron.*, vol. 18, no. 3–4, pp. 235–265, Jan. 2003.

[14] J. Chen, J. Huang, H. Lin, and Z. Pei, "Rice yield estimation by assimilation remote sensing into crop growth model," *SCI. CHINA Inf. Sci.*, vol. 40, pp. 173–183, 2010.

[15] L. Dente, G. Satalino, F. Mattia, and M. Rinaldi, "Assimilation of leaf area index derived from ASAR and MERIS data into CERES-Wheat model to map wheat yield," *Remote Sens. Environ.*, vol. 112, no. 4, pp. 1395–1407, Apr. 2008.

[16] H. Fang, S. Liang, G. Hoogenboom, J. Teasdale, and M. Cavigelli, "Corn-yield estimation through assimilation of remotely sensed data into the CSM-CERES-Maize model," *Int. J. Remote Sens.*, vol. 29, no. 10, pp. 3011–3032, 2008.

[17] H. Fang, S. Liang, and G. Hoogenboom, "Integration of MODIS LAI and vegetation index products with the CSM–CERES–Maize model for corn yield estimation," *Int. J. Remote Sens.*, vol. 32, no. 4, pp. 1039–1065, 2011.

[18] Y. Dong, J. Wang, C. Li, G. Yang, Q. Wang, and F. Liu *et al.*, "Comparison and analysis of data assimilation algorithms for predicting the leaf area index of crop canopies," *IEEE J. Sel. Top. Appl. Earth Observ. Remote Sens.*, vol. 6, no. 1, pp. 188–201, Feb. 2013.

[19] A. J. W. de Wit and C. A. van Diepen, "Crop model data assimilation with the Ensemble Kalman filter for improving regional crop yield forecasts," *Agric. Forest. Meteorol.*, vol. 146, no. 1–2, pp. 38–56, Sep. 2007.

[20] J. Wang, X. Li, L. Lu, and F. Fang, "Estimating near future regional corn yields by integrating multi-source observations into a crop growth model," *Eur. J. Agron.*, vol. 49, pp. 126–140, Aug. 2013.

[21] A. Monsivais-Huertero, W. D. Graham, J. Judge, and D. Agrawal, "Effect of simultaneous state-parameter estimation and forcing uncertainties on root-zone soil moisture for dynamic vegetation using EnKF," *Adv. Water Resour.*, vol. 33, no. 4, pp. 468–484, Apr. 2010.

[22] Q. Y. Duan, V. K. Gupta, and S. Sorooshian, "Shuffled complex evolution approach for effective and efficient global minimization," *J. Optim. Theory. Appl.*, vol. 76, no. 3, pp. 501–521, Mar. 1993.

[23] S. Kirkpatrick, C. D. Gelatt, and M. P. Vecchi, "Optimization by simulated annealing," *Science*, vol. 220, no. 4598, pp. 671–680, May 1983.

[24] M. J. D. Powell, "An efficient method for finding the minimum of a function of several variables without calculating derivatives," *Comput. J.*, vol. 7, no. 2, pp. 155–162, 1964.

[25] G. Evensen, "The Ensemble Kalman filter: Theoretical formulation and practical implementation," *Ocean Dyn.*, vol. 53, pp. 343–367, 2003.

[26] S. Arulampalam, S. Maskell, N. J. Gordon, and T. Clapp, "A tutorial on particle filters for online nonlinear/non-Gaussian Bayesian tracking," *IEEE Trans. Signal Process.*, vol. 50, no. 2, pp. 174–188, Feb. 2002.

[27] T. Rui, Q. Zhang, Y. Zhou, and J. Xing, "Object tracking using particle filter in the wavelet subspace," *Neurocomputing*, vol. 119, pp. 125–130, Nov. 2013.

[28] M. Leisenring and H. Moradkhani, "Snow water equivalent prediction using Bayesian data assimilation methods," *Stoch. Environ. Res. Risk Assess.*, vol. 25, no. 2, pp. 253–270, Feb. 2011.

[29] M. Leisenring and H. Moradkhani, "Analyzing the uncertainty of suspended sediment load prediction using sequential data assimilation," *J. Hydrol.*, vol. 468–469, pp. 268–282, Oct. 2012.

[30] C. Montzka, H. Moradkhani, L. Weihermüler, H. H. Franssen, M. Canty, and H. Vereecken, "Hydraulic parameter estimation by remotely-sensed top soil moisture observations with the particle filter," *J. Hydrol.*, vol. 399, no. 3–4, pp. 410–421, Mar. 2011.

[31] H. Moradkhani, C. M. DeChant, and S. Sorooshian, "Evolution of ensemble data assimilation for uncertainty quantification using the particle filter-Markov chain Monte Carlo method," *Water Resour. Res.*, vol. 48, no. 12, p. W12520, Dec. 2012.

[32] H. Moradkhani, K. Hsu, H. Gupta, and S. Sorooshian, "Uncertainty assessment of hydrologic model states and parameters: Sequential data assimilation using the particle filter," *Water Resour. Res.*, vol. 41, no. 5, p. W05012, May 2005.

[33] K. Nagarajan, J. Judge, W. D. Graham, and A. Monsivais-Huertero, "Particle filter-based assimilation algorithms for improved estimation of root-zone soil moisture under dynamic vegetation conditions," *Adv. Water Resour.*, vol. 34, no. 4, pp. 433–447, Apr. 2011.

[34] M. Pan, E. F. Wood, R. Wójcik, and M. F. McCabe, "Estimation of regional terrestrial water cycle using multi-sensor remote sensing observations and data assimilation," *Remote Sens. Environ.*, vol. 112, no. 4, pp. 1282–1294, Apr. 2008.

[35] J. Qin, S. Liang, K. Yang, I. Kaihotsu, R. Liu, and T. Koike, "Simultaneous estimation of both soil moisture and model parameters using particle filtering method through the assimilation of microwave signal," *J. Geophys. Res.*, vol. 114, p. D15103, Aug. 2009.

[36] J. van der Kwast, F. Canters, D. Karssenberg, G. Engelen, T. Van de Voorde, I. Uljee, and K. de Jong, "Remote sensing data assimilation in modeling urban dynamics: Objectives and methodology," *Proc. Environ. Sci.*, vol. 7, pp. 140–145, 2011.

[37] A. H. Weerts and G. Y. H. El Serafy, "Particle filtering and ensemble Kalman filtering for state updating with hydrological conceptual rainfall-runoff models," *Water Resour. Res.*, vol. 42, no. 9, p. W09403, Sep. 2006.

[38] M. G. de Kauwe, M. I. Disney, T. Quaife, P. Lewis, and M. Williams, "An assessment of the MODIS collection 5 leaf area index product for a region of mixed coniferous forest," *Remote Sens. Environ.*, vol. 115, no. 2, pp. 767–780, Feb. 2011.

[39] H. Fang, S. Wei, and S. Liang, "Validation of MODIS and CYCLOPES LAI products using global field measurement data," *Remote Sens. Environ.*, vol. 119, pp. 43–54, 2012.

[40] M. Claverie, V. Demarez, B. Duchemin, O. Hagolle, D. Ducrot, C. Marais-Sicre, J. Dejoux, M. Huc, P. Keravec, P. Béziat, R. Fieuzal, E. Ceschia, and G. Dedieu, "Maize and sunflower biomass estimation in southwest France using high spatial and temporal resolution remote sensing data," *Remote Sens. Environ.*, vol. 124, pp. 844–857, Sep. 2012.

[41] R. Savin, E. H. Satorre, A. J. Hall, and G. A. Slafer, "Assessing strategies for wheat cropping in the monsoonal climate of the Pampas using the CERES-Wheat simulation model," *Field Crops Res.*, vol. 42, no. 2–3, pp. 81–91, Aug. 1995.

[42] P. Dhungana, K. M. Eskridge, A. Weiss, and P. S. Baenziger, "Designing crop technology for a future climate: An example using response surface methodology and the CERES-Wheat model," *Agric. Syst.*, vol. 87, no. 1, pp. 63–79, Jan. 2006.

[43] X. Xiong, I. M. Navon, and B. Uzunoglu, "A note on the particle filter with posterior Gaussian resampling," *Tellus A*, vol. 58, no. 4, pp. 456–460, 2006.

[44] J. Yu, Y. Tang, and W. Liu, "An improved resampling algorithm in particle filter," *J. Comput. Inf. Syst.*, vol. 6, pp. 629–635, 2010.

[45] R. Douc and O. Cappe, "Comparison of resampling schemes for particle filtering," in *Proc. 4th Int. Symp. Image Signal Process. Anal. (ISPA)*, 2005, pp. 64–69.

[46] P. Salamon and L. Feyen, "Assessing parameter, precipitation, and predictive uncertainty in a distributed hydrological model using sequential data assimilation with the particle filter," *J. Hydrol.*, vol. 376, no. 3–4, pp. 428–442, Oct. 2009.

[47] N. J. Gordon, D. J. Salmond, and A. F. M. Smith, "Novel approach to nonlinear/non-Gaussian Bayesian state estimation," *IEE Proc. F Radar Signal Process.*, vol. 140, no. 2, pp. 107–113, Apr. 1993.

[48] J. S. Liu and R. Chen, "Sequential Monte Carlo methods for dynamic systems," *J. Amer. Stat. Assoc.*, vol. 93, no. 443, pp. 1032–1044, Sep. 1998.

[49] G. Kitagawa, "Monte Carlo filter and smoother for non-Gaussian nonlinear state space models," *J. Comput. Graph. Stat.*, vol. 5, no. 1, pp. 1–25, Mar. 1996.

[50] M. Dettori, C. Cesaraccio, A. Motroni, D. Spano, and P. Duce, "Using CERES-Wheat to simulate durum wheat production and phenology in Southern Sardinia, Italy," *Field Crops Res.*, vol. 120, no. 1, pp. 179–188, Jan. 2011.

[51] V. K. Arora, H. Singh, and B. Singh, "Analyzing wheat productivity responses to climatic, irrigation and fertilizer-nitrogen regimes in a semi-arid sub-tropical environment using the CERES-Wheat model," *Agric. Water Manage.*, vol. 94, no. 1–3, pp. 22–30, Dec. 2007.

[52] A. K. Singh, R. Tripathy, and U. K. Chopra, "Evaluation of CERES-Wheat and CropSyst models for water–nitrogen interactions in wheat crop," *Agric. Water Manage.*, vol. 95, no. 7, pp. 776–786, Jul. 2008.

[53] M. Mansouri, B. Dumont, and M. Destain, "Modeling and prediction of nonlinear environmental system using Bayesian methods," *Comput. Electron. Agric.*, vol. 92, pp. 16–31, Mar. 2013.

[54] C. Naud, D. Makowski, and M. Jeuffroy, "Application of an interacting particle filter to improve nitrogen nutrition index predictions for winter wheat," *Ecol. Modell.*, vol. 207, no. 2–4, pp. 251–263, Oct. 2007.

[55] J. M. Sabater, C. Rüdiger, J. Calvet, N. Fritz, L. Jarlan, and Y. Kerr, "Joint assimilation of surface soil moisture and LAI observations into a land surface model," *Agric. Forest Meteorol.*, vol. 148, no. 8–9, pp. 1362–1373, Jul. 2008.

[56] M. P. Clark, D. E. Rupp, R. A. Woods, X. Zheng, R. P. Ibbitt, A. G. Slater, J. Schmidt, and M. J. Uddstrom, "Hydrological data assimilation with the ensemble Kalman filter: Use of streamflow observations to update states in a distributed hydrological model," *Adv. Water Resour.*, vol. 31, no. 10, pp. 1309–1324, Oct. 2008.

[57] D. Ding, *Soil Species of Hebei Province*. Shijiazhuang, China: Hebei Sci. Technol. Press, 1992.

[58] F. H. Al-Sadah and F. M. Ragab, "Study of global daily solar radiation and its relation to sunshine duration in Bahrain," *Solar Energy*, vol. 47, no. 2, pp. 115–119, 1991.

[59] M. F. Hutchinson and T. Xu, *ANUSPLIN Version 4.36 User Guide*. Australian National Univ., 2013. Available: http://fennerschool.anu.edu.au/files/anusplin44.pdf

[60] Z. Cao, J. Yang, and M. Qiao, *Hebei Rural Statistic Yearbook*. Beijing, China: China Statistics Press, 2010.

[61] M. J. Canty, *Image Analysis, Classification, and Change Detection in Remote Sensing: With Algorithms for ENVI/IDL*, 2nd ed. Boca Raton, FL, USA: CRC Press, 2009.

[62] A. Kuusk, "A two-layer canopy reflectance model," *J. Quant. Spectrosc. Radiat. Transfer*, vol. 71, no. 1, pp. 1–9, Oct. 2001.

[63] B. He, X. Quan, and M. Xing, "Retrieval of leaf area index in alpine wetlands using a two-layer canopy reflectance model," *Int. J. Appl. Earth Observ. Geoinf.*, vol. 21, pp. 78–91, Apr. 2013.

[64] J. Chen, P. Jönsson, M. Tamura, Z. Gu, B. Matsushita, and L. Eklundh, "A simple method for reconstructing a high-quality NDVI time-series data set based on the Savitzky-Golay filter," *Remote Sens. Environ.*, vol. 91, no. 3–4, pp. 332–344, Jun. 2004.

[65] A. Savitzky and M. J. E. Golay, "Smoothing and differentiation of data by simplified least squares procedures," *Anal. Chem.*, vol. 36, no. 8, pp. 1627–1639, Jul. 1964.

[66] M. Jardak, I. M. Navon, and M. Zupanski, "Comparison of sequential data assimilation methods for the Kuramoto-Sivashinsky equation," *Int. J. Numer. Methods Fluids*, vol. 62, no. 4, pp. 374–402, Feb. 2010.

[67] A. M. Moore, H. G. Arango, G. Broquet, B. S. Powell, A. T. Weaver, and J. Zavala-Garay, "The regional ocean modeling system (ROMS) 4-dimensional variational data assimilation systems: Part I–system overview and formulation," *Prog. Oceanogr.*, vol. 91, no. 1, pp. 34–49, Oct. 2011.

[68] H. Moradkhani, S. Sorooshian, H. V. Gupta, and P. R. Houser, "Dual state-parameter estimation of hydrological models using ensemble Kalman filter," *Adv. Water Resour.*, vol. 28, no. 2, pp. 135–147, Feb. 2005.

[69] A. V. M. Ines, N. N. Das, J. W. Hansen, and E. G. Njoku, "Assimilation of remotely sensed soil moisture and vegetation with a crop simulation model for maize yield prediction," *Remote Sens. Environ.*, vol. 138, pp. 149–164, Nov. 2013.

[70] X. Tian, Z. Xie, and Q. Sun, "A POD-based ensemble four-dimensional variational assimilation method," *Tellus Ser. A*, vol. 63, no. 4, pp. 805–816, Aug. 2011.

[71] Y. Cao, J. Zhu, I. M. Navon, and Z. Luo, "A reduced-order approach to four-dimensional variational data assimilation using proper orthogonal decomposition," *Int. J. Numer. Methods Fluids*, vol. 53, pp. 1571–1583, 2007.
[72] C. Qiu, L. Zhang, and A. Shao, "An explicit four-dimensional variational data assimilation method," *Sci. China Ser. D Earth Sci.*, vol. 50, no. 8, pp. 1232–1240, Aug. 2007.
[73] J. L. Champeaux, V. Masson, and F. Chauvin, "ECOCLIMAP: A global database of land surface parameters at 1 km resolution," *Meteorol. Appl.*, vol. 12, pp. 29–32, 2005.
[74] S. Plummer, O. Arino, F. Ranera, K. Tansey, C. Jing, G. Dedieu, H. Eva, I. Piccolini, R. Leigh, G. Borstlap, B. Beusen, W. Heyns, and R. Benedetti, "The GLOBCARBON initiative global biophysical products for terrestrial carbon studies," in *Proc. IEEE Int. Geosci. Remote Sens. Symp. (IGARSS)*, Barcelona, Spain, 2007, pp. 2408–2411.
[75] W. Yang, B. Tan, D. Huang, M. Rautiainen, N. V. Shabanov, Y. Wang *et al.*, "MODIS leaf area index products: From validation to algorithm improvement," *IEEE Trans. Geosci. Remote Sens.*, vol. 44, no. 7, pp. 1885–1898, Jul. 2006.
[76] Y. Yao, Q. Liu, Q. Liu, and X. Li, "LAI retrieval and uncertainty evaluations for typical row-planted crops at different growth stages," *Remote Sens. Environ.*, vol. 112, no. 1, pp. 94–106, Jan. 2008.

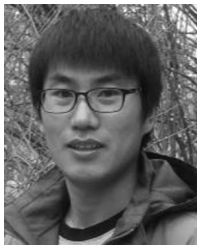

Zhiwei Jiang received the B.S. degree in resources environment and urban planning management from the Inner Mongolia Normal University, Hohhot, China, in 2006, the M.Sc. degree in environmental science from the Capital Normal University, Beijing, China, in 2009, and the Ph.D. degree in agricultural remote sensing from the Chinese Academy of Agricultural Sciences, Beijing, China, in 2012.

Currently, he is engaged in postdoctoral research work in cartography and geographic information systems with the Beijing Normal University, Beijing, China, and the Chinese Academy of Agricultural Sciences. His research interests include agricultural remote sensing, crop growth simulation, and data assimilation.

Zhongxin Chen received the B.S. degree in physical geography from Peking University, Beijing, China, in 1991, and the M.Sc. and Ph.D. degrees in ecology from the Chinese Academy of Science, Beijing, China, in 1994 and 1998, respectively.

Currently, he is a Researcher with the Institute of Agricultural Resources and Regional Planning, Chinese Academy of Agricultural Sciences, Beijing, China. His research interests include remote sensing application in agriculture, spatial modeling, and agricultural information technology. He has published more than 100 articles in the academic journals.

Jin Chen received the B.A. and M.S. degrees in geography from Beijing Normal University, Beijing, China, in 1989 and 1992, respectively, and the Ph.D. degree in civil engineering from Kyushu University, Fukuoka, Japan, in 2000.

He was a Postdoctoral Researcher with the University of California, Berkeley, CA, USA, from 2000 to 2001, and with the National Institute of Environmental Studies, Tsukuba, Japan, from 2001 to 2004. Currently, he is a Professor with the College of Global Change and Earth System Science, Beijing Normal University. His research interests include remote sensing modeling and vegetation parameter retrieval through the inversion of remote sensing models. He has published more than 80 papers in international journals with citation numbers of more than 900.

Jia Liu received the B.Eng. degree in automatic control from the Beijing Institute of Technology, Beijing, China, in 1990, and the M.Eng. degree in fluid power transmission and hydraulic control from the China Academy of Launch Vehicle Technology, Beijing, China, in 1993.

Currently, she is an Associate Researcher with the Institute of Agricultural Resources and Regional Planning, Chinese Academy of Agricultural Sciences, Beijing, China. Her research interests include crop identification and target extraction.

Jianqiang Ren received the B.S. degree in soil science, the M.S. degree in management of land resources from Hebei Agricultural University, Hebei, China, in 2000 and 2003, respectively, and the Ph.D. degree in agricultural remote sensing from China Agricultural University, Beijing, China, in 2006.

Currently, he is an Associate Professor with the Institute of Agricultural Resources and Regional Planning, Chinese Academy of Agricultural Sciences, Beijing, China. His research interests include applications of agricultural remote sensing, crop growth monitoring, crop yield simulation and forecasting, critical crop parameter retrieval, and data assimilation. He has published more than 30 peer-reviewed research papers in scientific journals.

Zongnan Li received the B.S. degree in resources environment and urban planning management from the Hunan Agricultural University, Changsha, China, in 2006, and the M.Sc. degree in agricultural remote sensing from the Chinese Academy of Agricultural Sciences, Beijing, China, in 2010.

Currently, he is working toward the Ph.D. degree in agricultural remote sensing in the Chinese Academy of Agricultural Sciences. His research interests include applications of agricultural remote sensing, hyperspectral applications, crop growth monitoring, and agro-ecology.

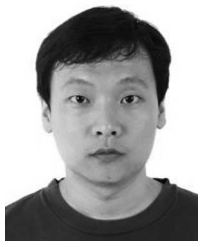

Liang Sun received the B.S. degree in land resources management from the China University of Geoscience, Beijing, China, in 2005, and the M.S. and Ph.D. degrees in remote sensing from the Beijing Normal University, Beijing, China, in 2007 and 2010, respectively.

His research interests include evapotranspiration, soil moisture, and agricultural remote sensing.

He Li received the B.S. degree in geographic information systems from the Xinjiang University, Urumchi, China, in 2009, and the M.Sc. degree in cartography and geographic information system from the Hohai University, Nanjing, China, in 2012. Currently, he is working toward the Ph.D. degree in agricultural remote sensing at the Chinese Academy of Agricultural Sciences, Beijing, China.

His interests include agricultural remote sensing, crop evapotranspiration, and data assimilation.